A Kirkwood−Buff Derived Force Field for Mixtures of Urea and Water

Samantha Weerasinghe[†] and Paul E. Smith*

Department of Biochemistry, Kansas State University, Manhattan, Kansas 66506-3702

Received: September 12, 2002; In Final Form: January 28, 2003

A new nonpolarizable force field for mixtures of urea and water is described. The model was parametrized to reproduce the experimental Kirkwood−Buff integrals between urea−urea, urea−water, and water−water pairs, as defined by the Kirkwood−Buff theory of solution mixtures. It was observed that the integrals were sensitive to the charge distribution used, and that none of the literature charge distributions investigated produced the correct degree of urea association. However, a hybrid charge distribution was found which accurately reproduced the integrals over a range of concentrations. Correspondingly, the solution thermodynamics, including the activity of urea, were well described. In addition, other physical properties (density, diffusion constants, compressibility) were also well reproduced. The model displayed little or no urea self-aggregation, in agreement with the experimental data. The ideal nature of urea mixtures (molar activity scale) appeared to result from a balance between water−water and urea-water interactions, with a smaller urea−urea interaction. Although developed for use with SPC/E water, the new model performed equally well with the SPC and TIP3P water models.

Introduction

Protein denaturation by urea is consistently used by experimentalists to study the stability of proteins and the nature of the denatured state. Unfortunately, the exact details of the mechanism by which urea favors the unfolded form remain unclear. However, the dentauration process is known to be at least partially dependent on the thermodynamic properties of urea and water mixtures, and the solution activities in particular.[1−3] One possible way to further our knowledge of urea denaturation is to use computer simulation.[4−7] To study urea denaturation by simulation one requires a urea and water force field which reproduce the appropriate experimental data. While several urea force fields exist,[4,8−14] the activity of urea in solution has not been determined for any of the models. This is mainly due to the small associated changes in the chemical potential of urea with concentration, which would require the determination of very precise solvation free energies for urea.

Most current force fields are derived by combining (scaled or fitted) ab initio derived charge distributions with the appropriate repulsion, dispersion, and nonbonded parameters. The force fields are then usually validated by examining the properties (density, radial distribution functions, dielectric constant, diffusion constant, compressibility, etc.) of mixtures with water. There are several urea force fields available using this type of approach.[10−12] Recent tests and comparisons of different urea force fields also exist.[15,16] One of these studies demonstrated a model-dependent range of urea self-aggregation in solution, which could have implications for the mechanism of urea denaturation.[16] However, no firm conclusions could be drawn concerning which model best reproduces the experimental data because that the degree of urea aggregation is unknown and the subject of some debate.[17] Clearly, one desires a model which reproduces the correct degree of urea self-association as a function of concentration.

* Corresponding author. Fax: 785-532-7278. E-mail: pesmith@ksu.edu.
[†] Permanent address: Department of Chemistry, University of Ruhuna, Matara, Sri Lanka.

While the solution activity is difficult to obtain directly, it is possible to obtain derivatives of the urea activity without determining chemical potentials. Solution activity derivatives can be extracted from simulations by use of the Kirkwood−Buff (KB) theory of solutions, which relates thermodynamic data to integrals over pair distributions in solution.[18] The theory provides a direct link between urea aggregation and urea activity derivatives. Here, we have used KB theory to develop a urea force field (KBFF) which reproduces the experimentally determined KB integrals as a function of urea concentration.[17] Hence, the thermodynamic properties, including the activity of the solution, are well reproduced. It is also shown that this is not necessarily true for previous models. The model is designed to be used with the SPC/E model for water,[19] which we consider to represent a good compromise between efficiency and accuracy. However, good results are also obtained for the SPC[20] and TIP3P[21] three site models. Inclusion of explicit polarization effects was not considered here as the force field is intended for the study of urea denaturation of proteins and most common protein force fields do not currently include polarization.

Methods

Molecular Dynamics Simulations. The different urea solutions reported here were simulated using classical molecular dynamics techniques. Several water models were examined (SPC/E, SPC, TIP3P), although the majority of simulations involved the SPC/E model. All simulations were performed in the isothermal isobaric ensemble at 300 K and 1 atm. The weak coupling technique[22] was used to modulate the temperature and pressure with relaxation times of 0.1 and 0.5 ps, respectively. All bonds were constrained using SHAKE[23] and a relative tolerance of 10^{-4}, allowing a 2 fs time step for integration of the equations of motion. The particle mesh Ewald technique was used to evaluate electrostatic interactions.[24,25] A real space convergence parameter of 3.5 nm^{-1} was used in combination with twin range cutoffs of 0.8 and 1.5 nm, and a nonbonded update frequency of 10 steps. The reciprocal space sum was

10.1021/jp022049s CCC: $25.00
Published on Web 04/01/2003

evaluated on a 40^3 grid with ≈0.1 nm resolution. Initial configurations of the different solutions were generated from a cubic box ($L \approx 4.0$ nm) of equilibrated water molecules by randomly replacing waters with urea until the required concentration was attained. The steepest descent method was then used to perform 100 steps of minimization. This was followed by extensive equilibration which was continued until all inter species potential energy contributions displayed no drift with time. Total simulation times were in the 2−3 ns range, and the final 2.5 ns were used for calculating ensemble averages. Configurations were saved every 0.1 ps for the calculation of various properties. Errors ($\pm 1\sigma$) in the simulation data were estimated by using two or three block averages. Diffusion constants were determined using the mean square fluctuation approach,[26] relative permittivities from the dipole moment fluctuations,[27] and compressibilities by performing a finite difference calculation using additional simulations of 250 ps at 1000 atm. Relaxation times were obtained after fitting the appropriate correlation function (first-order Legendre polynomial) to a single-exponential decay model.[28]

Kirkwood−Buff Theory. The development of KB theory is described in detail elsewhere.[18,29] The thermodynamic properties of a solution mixture can be expressed in terms of the KB integrals between the different solution components. Hence, for a binary solution consisting of water (w) and urea (u), a variety of thermodynamic quantities can be defined in terms of the integrals G_{ww}, G_{uu}, and G_{uw}, and the number densities (or molar concentrations) ρ_w and ρ_u. The partial molar volumes of the two components, $\bar{V}$; the isothermal compressibility of the solution, κ_T; derivatives of the chemical potential, μ; derivatives of the urea molar activity, $a_u = y_u\rho_u$; and derivatives of the urea mole fraction scale activity coefficients, f_u, at a pressure (p) and a temperature (T) are given by[29]

$$\bar{V}_w = \frac{1 + \rho_u(G_{uu} - G_{uw})}{\eta}; \; \bar{V}_u = \frac{1 + \rho_w(G_{ww} - G_{uw})}{\eta}; \quad \kappa_T = \frac{\beta\zeta}{\eta} \tag{1}$$

$$a_{uu} = \left(\frac{\partial \ln a_u}{\partial \ln \rho_u}\right)_{p,T} = 1 + \left(\frac{\partial \ln y_u}{\partial \ln \rho_u}\right)_{p,T} = \frac{1}{1 + \rho_u(G_{uu} - G_{uw})} \tag{2}$$

$$f_{uu} = \left(\frac{\partial \ln f_u}{\partial \ln x_u}\right)_{p,T} = -\frac{\rho_w x_u(G_{ww} + G_{uu} - 2G_{uw})}{1 + \rho_w x_u(G_{ww} + G_{uu} - 2G_{uw})} \tag{3}$$

where $\eta = \rho_w + \rho_u + \rho_w\rho_u(G_{ww} + G_{uu} - 2G_{uw})$, $\zeta = 1 + \rho_w G_{ww} + \rho_u G_{uu} + \rho_w\rho_u(G_{ww}G_{uu} - G_{uw}^2)$, $\beta = 1/(RT)$, and R is the gas constant. For real (stable) solutions the values of η and ζ must be positive.[29] No approximations are made during the derivation.

The above thermodynamic properties are expressed in terms of KB integrals which are defined as[18]

$$G_{ij} = 4\pi \int_0^\infty [g_{ij}^{\mu VT}(r) - 1]\, r^2\, dr \tag{4}$$

Here, G_{ij} is the KB integral between species i and j, $g_{ij}^{\mu VT}(r)$ is the corresponding radial distribution function (rdf) in the μVT ensemble, and r is the distance between the centers of mass of the two species. KB integrals were determined from the simulation data (NpT ensemble) by assuming that

$$G_{ij} = 4\pi \int_0^R [g_{ij}^{NpT}(r) - 1]\, r^2\, dr \tag{5}$$

where R represents a correlation region within which the solution composition differs from the bulk composition.[29] All rdfs are assumed to be unity beyond R. Excess coordination numbers are defined as $N_{ij} = \rho_j G_{ij}$. A value of N_{ij} greater than zero indicates an excess of species j in the vicinity of species i (over a random distribution), while a negative value corresponds to a depletion of species j surrounding i. Hence, KB theory provides a direct relationship between urea self-aggregation (N_{uu}) and urea activity derivatives through eq 2, and should provide a good test of a particular force field. In practice, a slightly larger simulation volume than usual is required in order to ensure that the rdfs approach unity at large distances. Our previous simulations have indicated that a combination of KB theory and NpT simulations can provide quantitative information concerning the thermodynamics of solutions.[15,30,31] In addition, we have recently extracted the experimental KB integrals for urea solutions at 300 K and 1 atm by inversion of the KB approach.[17]

Parameter Development. The experimental geometry for urea was used to determine equilibrium bond lengths and angles.[32] Force constants for the bonded terms were taken from the GROMOS96 force field.[33] Nonbonded interactions were described by the commonly used Lennard-Jones 6−12 potential combined with a Coulomb potential. Geometric combination rules were used for both the 6−12 σ and ϵ parameters. During our initial investigations into the properties of urea solutions it was observed that the KB parameters were relatively insensitive to reasonable variations in the σ (± 0.01 nm) and ϵ (± 0.1 kJ/mol) parameters. They were, however, very sensitive to the partial charge distribution used for urea. Interestingly, the integrals varied more with changes in the charge distribution than with simple scaling of all the charges, and the urea model dipole moment was not a good indicator of urea solvation or aggregation.[34]

Considering the above observations, the σ and ϵ parameters were determined by reference to the work of Miller and Savchik who demonstrated a correlation between atomic size and atomic hydrid components (τ_i) of molecular polarizabilities.[35] Values of τ depend on hybridization and not connectivity. Furthermore, it was assumed that the form of the dispersion interaction followed the London equation.[36] Hence, our values of σ_{ii} and ϵ_{ii} were taken to be proportional to $\tau_i^{1/2}$ and $\tau_i I_i$, respectively. The scaling factor for ϵ (0.0207) was determined by reference to the value of the SPC/E water oxygen, with hybridization-dependent ionization potentials (I) taken from Hinze and Jaffe.[37] The scaling factor for σ (0.281 for the final charge distribution) was then varied to obtain a reasonable solution density for a particular charge distribution. Several literature charge distributions were investigated.[9,13,38] A good compromise between the charges of Dovesi et al. ($q_O = -0.770$, $q_C = 1.180$, $q_N = -0.745$, $q_H = 0.270$),[38] which displayed too little aggregation, and the OPLS charges ($q_O = -0.390$, $q_C = 0.142$, $q_N = -0.542$, $q_H = 0.333$),[9] which displayed too much aggregation, was found to be given by $q = q_{OPLS} + 0.75(q_D - q_{OPLS})$. The corresponding dipole moment of a single urea molecule was 4.65 D, compared to the experimental values of 4.6, 4.4, and 5.7 D for urea in dioxane, acetone, and water, respectively.[39] The final force field parameters are displayed in Tables 1 and 2, and a summary of the simulations performed is presented in Table 3.

Results

The rdfs and corresponding KB integrals as a function of interatomic distance are displayed in Figure 1 for an 8 M urea solution. The urea−urea rdf displayed some structure to distances of 1.2 nm. The structure observed in the rdfs was

TABLE 1: Bonded Parameters for KBFF Urea[a]

bonds	C−O	C−N	N−H
r_o	0.1265	0.1350	0.1000
angles	**O−C−N**	**N−C−N**	**C−N−H**	**H−N−H**
k_θ	730.0	670.0	390.0	445.0
θ_o	121.4	117.2	120.0	120.0
dihedrals	**O−C−N1−H**	**O−C−N2−H**
k_ϕ	33.5	33.5
δ	−180	−180
n	2	2
impropers	**C−O−N1−N2**	**N−H1−H2−C**
k_ω	167.4	167.4
ω_o	0.0	0.0

[a] Potential functions are the following: angles, $V_\theta = {}^1/_2 k_\theta(\theta - \theta_o)^2$; dihedrals, $V_\phi = k_\phi[1 + \cos(n\phi - \delta)]$; and impropers, $V_\omega = {}^1/_2 k_\omega(\omega - \omega_o)^2$. Energies (force constants) are in kJ/mol, angles in degrees, and distances in nm. Bond lengths were constrained using SHAKE.

TABLE 2: Final Nonbonded Parameters[a]

model	atom	ϵ (kJ/mol)	σ (nm)	q ($\|e\|$)
		Urea		
KBFF	C	0.417	0.377	0.921
	O	0.560	0.310	−0.675
	N	0.500	0.311	−0.693
	H	0.088	0.158	0.285
		Water		
SPC/E	O	0.6506	0.3166	−0.8476
	H	0.0000	0.0000	0.4238

[a] Combination rules: $\sigma_{ij} = \sqrt{\sigma_{ii}\sigma_{jj}}$ and $\epsilon_{ij} = \sqrt{\epsilon_{ii}\epsilon_{jj}}$.

TABLE 3: Summary of the MD Simulations of Urea Solutions[a]

N_u	N_w	x_u	ρ_u (M)	m_u (mol/kg)	V (nm^3)	ρ (g/cm^3)	T_{sim} (ns)
0	2170	0.0000	0.00	0.00	65.265	0.995	2
77	1941	0.0382	2.00	2.20	64.059	1.026	3
154	1750	0.0809	3.99	4.88	64.018	1.057	3
231	1557	0.1292	6.00	8.24	63.923	1.089	3
308	1362	0.1844	8.02	12.55	63.737	1.121	3

[a] Symbols are: N_i, number of i molecules; m_u, urea molality; V, average simulation volume; and T_{sim}, total simulation time. All simulations were performed at 300 K and 1 atm.

magnified in the KB integrals which indicated variations in the pair distributions even at larger distances of 1.5 nm. The oscillations in the KB integrals were clearly due to packing requirements for the molecules and displayed a period length of around 0.35 nm at large R. For this reason, the appropriate KB integral values were obtained after averaging the data between 0.95 and 1.30 nm. The results are displayed as lines in Figure 1. Consequently, some error in the value of the integrals was introduced (±10 cm^3/mol), but this is on the order of the error in the experimental data.[17] Values of G_{uu} displayed the largest errors, especially at low urea concentrations, due to the smaller number of molecules involved in determining g_{uu}. The convergence properties of the KB integrals as a function of simulation time are displayed in Figure 2. Reasonable values of the KB integrals were obtained after 1 ns, although there were some small variations in the values even after 2 ns, with G_{uu} displaying the largest deviations. All the data quoted here correspond to KB integrals determined from 2.5 ns of simulation and averaged between 0.95 and 1.30 nm. First shell coordination numbers obtained from the rdfs are presented in Table 4 and indicated gradual changes in coordination with concentration,

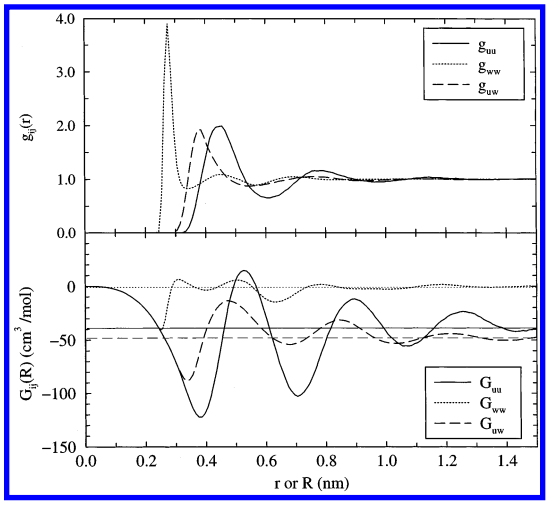

Figure 1. Radial distribution functions and Kirkwood−Buff integrals as a function of distance for 8 M urea. The straight lines correspond to the values of the KB integrals after averaging between 0.95 and 1.3 nm (see Methods section).

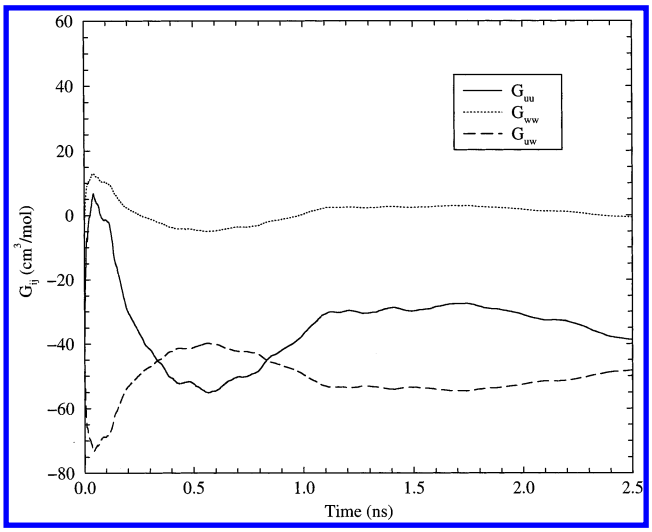

Figure 2. Kirkwood−Buff integrals in 8 M urea as a function of simulation time.

TABLE 4: First Shell Coordination Numbers

ρ_u (M)	urea−urea	urea−water	water−water
0.00			4.7
2.00	1.2	21.4	4.5
3.99	2.3	19.4	4.2
6.00	3.4	17.5	3.9
8.02	4.5	15.4	3.6

[a] The distance to the first minimum of the rdf was 0.615 nm for urea−urea, 0.565 nm for urea−water, and 0.335 nm for water−water. Errors were typically ±0.1.

as observed previously.[26] We have chosen not to compare the atom-based rdfs obtained here with the experimental data[40] due to the problems associated with decoupling site−site contributions for polyatomic molecules.

The KB integrals as a function of urea concentration are displayed in Figure 3 as excess coordination numbers. Two sets of experimental activity derivatives are available in the literature,[41,42] leading to two slightly different sets of KB integrals,[17] and thus providing an indication of possible experimental errors. The KBFF model reproduced the experimental data almost exactly, with some small errors at low (2 M) concentrations. The values obtained for the popular OPLS urea force field[9] are also included in Figure 3 to illustrate that the KB integrals are

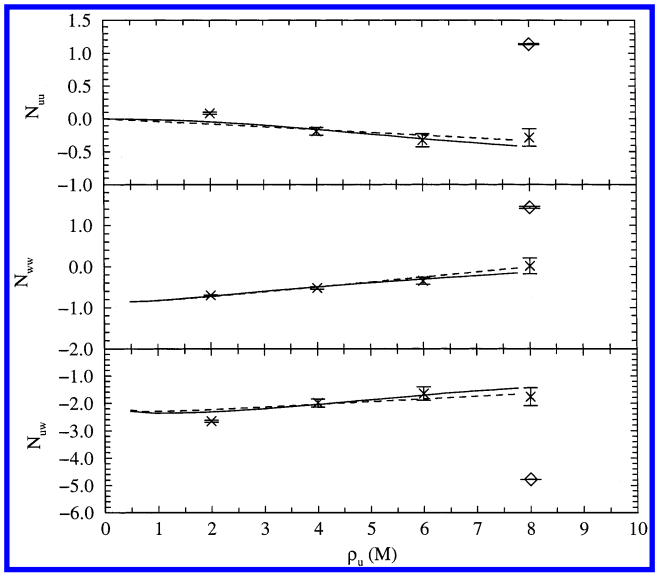

Figure 3. Excess coordination numbers for mixtures of urea and water. Lines represent the experimental data,[17] crosses correspond to the KBFF model, and diamonds are for the OPLS/TIP3P model.

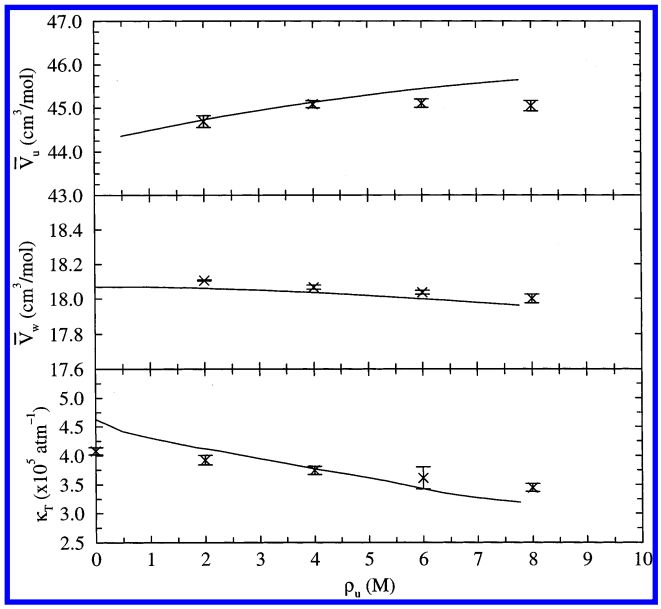

Figure 4. Partial molar volumes and isothermal compressibilities as a function of urea concentration. Lines represent the experimental data,[52,53] and crosses correspond to the KBFF model.

not reproduced naturally by all models. Values of G_{uu} and G_{uw} were -39 and -48 cm^3/mol for the current model at 8 M compared to the average experimental values of -48 and -42 cm^3/mol, respectively. Similar values for G_{uu} and G_{uw} are essential for ideal solution behavior (see eq 2). When these two integrals are equal, the molar activity derivative is close to unity. In fact, experimentally one observes that $G_{uu} \approx G_{uw} \approx \bar{V}_u \approx -45$ cm^3/mol for larger urea concentrations, which indicates that urea merely occupies a fixed amount of space and does not significantly attract other urea or water molecules.[43] In contrast, many alcohols display large degrees of aggregation with values of $G \approx 100-1000$ cm^3/mol.[44] The correct trends in excess coordination numbers with concentration were observed for the KBFF model.

The partial molar volumes and compressibilities are displayed in Figure 4. The agreement between the KBFF model and experiment was excellent. Consistently larger water partial molar volumes were obtained due to the slightly lower than experimental density exhibited by the SPC/E model. However, larger deviations in densities have been observed for other models.[16] The isothermal compressibilities were obtained from finite difference calculations as the values of $RT\,\kappa_T$ are small ($\approx$1 cm^3/mol) and therefore less than the precision of the current simulated KB integrals. Compressibilities were well reproduced but were less dependent on concentration than the experimental data. In all cases, the KBFF model reproduced the correct experimental trends with increasing urea concentration. Most importantly, the correct trends and magnitudes were observed for the two activity derivatives, a_{uu} and f_{uu}, indicating that the solution activity would be correctly reproduced on integration of these derivatives. This is demonstrated in Figure 5 where the molar and mole fraction scale activity coefficients are displayed. The coefficients were determined by assuming that $\ln f_u = \alpha(x_u^2 - 2x_u)$ for urea solutions, as suggested by Miyawaki et al.,[42] and then obtaining α from a fit to the MD derived derivatives ($\alpha_{exp} = 0.8309$ and $\alpha_{MD} = 1.09$). The molar activity coefficient was then obtained using standard conversion procedures.[45] The simulation results were in very good agreement with the experimental data.

TABLE 5: Relaxation Times and Relative Permittivities[a]

ρ_u (M)	τ_u (ps)	τ_w (ps)	τ_M (ps)	ϵ
0.00		6.0	9	72
2.00	10	6.5	10	70
3.99	11	7.5	16	75
6.00	14	8.8	20	68
8.02	15	11.5	21	69

[a] Symbols: τ_u and τ_w, single molecule rotational relaxation times for the urea and water dipoles, respectively; τ_M, total dipole moment relaxation time; ϵ, relative permittivity.

The density, relative permittivities, and diffusion constants of urea and water mixtures are displayed in Figure 6. The variation in density was well reproduced by the model, although this was used as an indicator during the parametrization. The urea diffusion constant was not used for parametrization and it is therefore encouraging to see that the available experimental data were reproduced almost exactly. The simulated permittivities were slightly low, although these values are difficult to obtain with high precision. Furthermore, a direct comparison of permittivities is complicated by the fact that the dielectric constant of SPC/E water is lower than experiment.[46] The KBFF model did not reproduce the experimental increase in permittivity with concentration, the value remaining essentially constant. However, this is an improvement over other models which generally display a significant decrease.[26] Also shown in Table 5 are rotational and dielectric relaxational times determined from the simulations. All relaxation times increased with urea concentration, indicating a steady reduction in the dynamics of the system, probably due to a simple crowding effect.

In an effort to investigate the sensitivity of the results to a particular urea or water model, a comparison of the KBFF and OPLS models with different water models was performed. The results are shown in Table 6 for an 8 M urea solution. The KB integrals and activity derivatives were relatively insensitive to the water model used with the KBFF urea model. In fact, the KB integrals were better reproduced with both the SPC and TIP3P water models, although the solution densities were low. The OPLS/TIP3P model resulted in too much urea self-aggregation (positive G_{uu}) which was compounded by use of the SPC/E model. Hence, the values of a_{uu} were 3 to 6 times too small and therefore not representative of an ideal solution.

The reasons for the differences in the two models are obviously related to the relative interaction strengths between

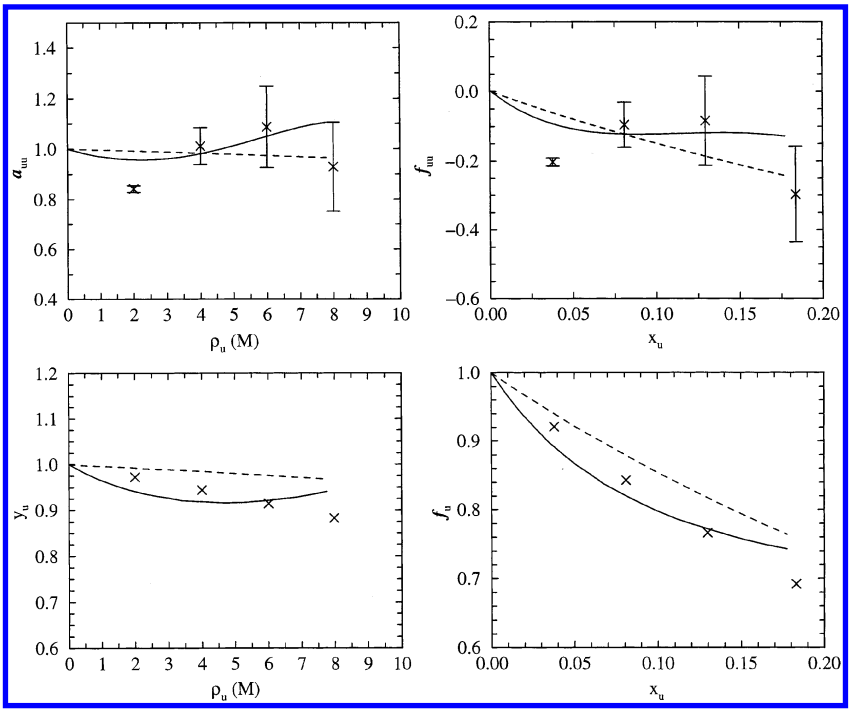

Figure 5. Activity derivatives and activity coefficients as a function of urea concentration. Lines represent the experimental data,[41,42] and crosses correspond to the KBFF model.

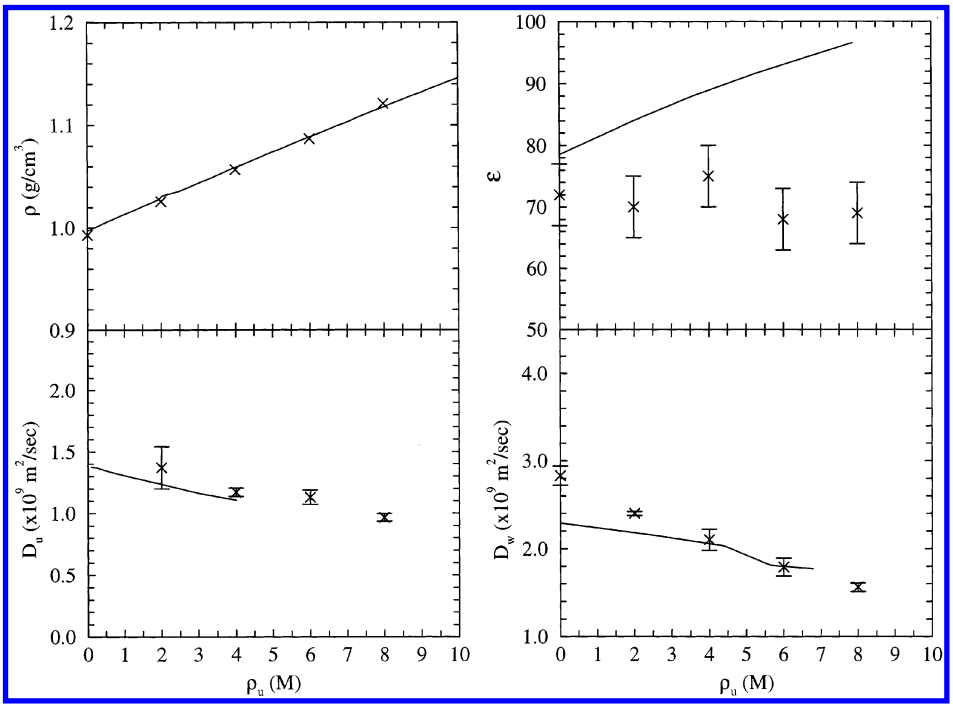

Figure 6. Density, relative permittivity, and diffusion constants as a function of urea concentration. Lines represent the experimental data,[48−51] and crosses correspond to the KBFF model.

the different molecules in solution. These interactions have been investigated by analyzing the pair interaction energies between the different species. The results are displayed in Figure 7. According to the pair energy distribution, the OPLS/TIP3P model displayed larger urea−urea and smaller urea−water interactions compared to the KBFF model. After decomposing into average distance-dependent interaction energies a slightly different picture emerges. Both models displayed similar average contact interaction energies between water−water and urea−water pairs. However, the urea−urea average contact interaction was substantially larger (−20 kJ/mol) for the OPLS/TIP3P model compared to the KBFF model (−8 kJ/mol), which helps to explain the larger degree of observed urea self-association.

Dipole−dipole distance correlation functions are also displayed in Figure 7 and help to define the interaction geometry between urea pairs. No dominant urea−urea interaction geometries were observed for the KBFF model due to the relatively weak self-interaction. The most populated geometries were defined by; $E_{ij} \approx -8$ kJ/mol, $R_{ij} \approx 0.4$ nm, and a dipole−dipole angle of $\approx 100°$. Configurations from the simulations which satisfied the above constraints typically involved stacked urea molecules with a slight tilt to favor an H to O electrostatic

TABLE 6: Comparison of the Properties of Different Models for 8 M Urea Solution[a]

	KBFF			OPLS			
property	SPC/E	SPC	TIP3P	SPC/E	TIP3P	exp[b]	units
ρ	1.121	1.104	1.108	1.130	1.118	1.119	g/cm^3
D_u	1.0	1.5	1.9	1.1	1.8		$\times 10^{-9}$ m^2/s
D_w	1.5	2.4	3.3	2.2	3.8		$\times 10^{-9}$ m^2/s
ϵ	69	62	78	63	61	95	
G_{uu}	−39	−51	−29	391	142	−53/−42	cm^3/mol
G_{uw}	−48	−41	−53	−282	−134	−40/−44	cm^3/mol
G_{ww}	−1	−5	1	128	41	−4/−1	cm^3/mol
a_{uu}	0.93	1.08	0.84	0.16	0.32	1.11/0.96	
f_{uu}	−0.30	−0.14	−0.33	−0.88	−0.78	−0.13/−0.25	

[a] See text for definitions; Typical errors are shown in Figures 3 to 5. [b] Two sets of experimental data exist for the activity of urea solutions, leading to two sets of KB integrals. Experimental data was taken from refs 17, 48−51.

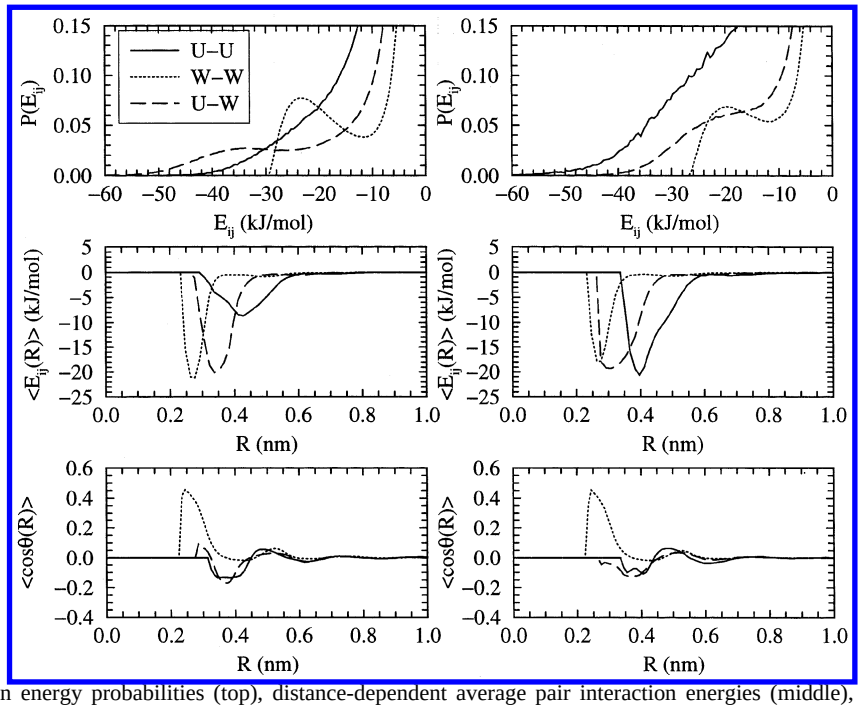

Figure 7. Pair interaction energy probabilities (top), distance-dependent average pair interaction energies (middle), and dipole−dipole spatial correlation functions (bottom) in 8 M urea solution for the KBFF model (left) and the OPLS/TIP3P model (right). θ is the angle between molecular dipoles.

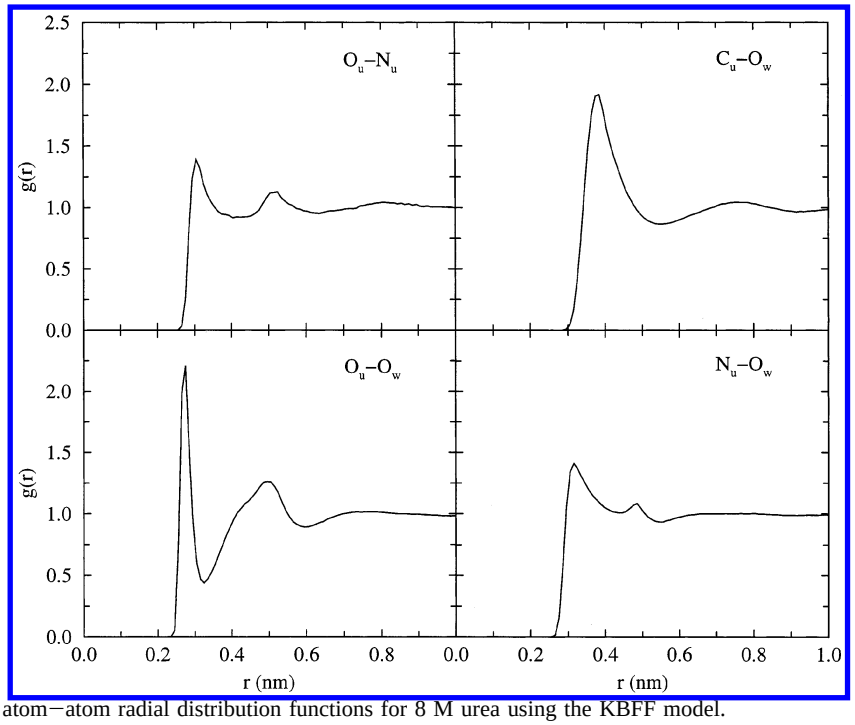

Figure 8. Intermolecular atom−atom radial distribution functions for 8 M urea using the KBFF model.

interaction (N−O = 0.31 nm and H−O of 0.24 nm). Similar structures were observed during the OPLS/TIP3P simulations. The larger interaction energy for this model was probably due to the smaller repulsive carbon-to-carbon electrostatic energy (see Table 2). Some of the atom-based rdfs for the KBFF model are displayed in Figure 8. Clearly, only a small interaction was apparent between the N and O atoms of urea, while the model displayed a large solvation of the urea oxygen by water. This behavior follows that expected due to the small hydrogen charges on urea compared to those on water (see Table 2).

For completion, the crystal structure of urea was simulated using the KBFF model. Although not designed for this purpose, large deviations would be an indication of any serious problems with the relative atomic sizes or the charge distribution. The simulated average unit cell dimensions at 123 K were $a = 0.527$ nm, $b = 0.526$ nm, and $c = 0.476$ nm for a $6 \times 6 \times 6$ unit cell simulation with anisotropic pressure scaling ($\alpha = \beta = \gamma = 90°$). The corresponding experimental dimensions are $a = b = 0.558$ nm and $c = 0.469$ nm.[32] The c dimension (head-to-tail arrangement of urea) was well reproduced. However, significant errors were observed for the a/b directions, leading to a 10% drop in the unit cell volume. The agreement with experiment is satisfactory for the KBFF force field as it is a relatively simplistic interaction potential compared to those designed to specifically study crystals and crystal interfaces,[13] and the results are as good as for other force fields.[47] It should be noted that none of the charge distributions investigated here could reproduce the crystal dimensions exactly. In particular, a consistent underestimation of the a/b dimension was observed, and in some cases the $a = b$ symmetry was also broken.

Conclusions

It has been shown that a realistic model for urea and water mixtures can be obtained by using a combination of molecular simulation and Kirkwood−Buff theory. The KB integrals were observed to be most sensitive to the charge distribution employed, and the urea dipole moment was not a good indicator of changes in the integrals. The results suggest that a KB analysis of water mixtures would be an objective way to distinguish between several different solute models. The main advantages of the KB approach are the direct relationship between the atomic level distribution functions and the thermodynamic data, and that the distributions are easily obtained from simulation. The major disadvantages are the requirement of larger systems to allow the KB integrals to plateau with distance ($g_{ij} = 1$), and the time required to reach convergence (1−2 ns). The latter is particularly problematic for parameter optimization. However, these problems will be significantly reduced with continued increases in computer power.

The urea model developed here reproduced the experimentally determined urea activity changes. The fact that G_{uu} and G_{uw} are small and negative indicates that (i) the molar activity is relatively constant resulting in almost ideal behavior, and (ii) urea aggregation is negligible as defined by $N_{uu} = \rho_u G_{uu}$. The latter being particularly insignificant in comparison with the aggregation observed for other solution mixtures. The consequences of these conclusions have been discussed in detail elsewhere.[17] Analysis of the simulations suggested that the reason for the ideal behavior of urea solutions arises from the similar average interaction energies between water molecules and urea and water molecules, with a smaller average urea self-interaction energy.

Finally, we note that it is possible that one of the models not investigated here could reproduce the experimental KB integrals, or that a different charge distribution could perform equally as well as the one adopted here. However, several of the other urea models display urea aggregation which is larger than that for OPLS.[16] More importantly, as none of the ab-initio derived charge distributions tested here were successful, and simple charge scaling did not improve the results, we feel it is possible that gas-phase-derived charge distributions may not accurately represent the polarized solution charge distributions. Variation of the charge distribution in order to obtain the correct KB integrals may provide a more appropriate approach. Alternatively, one could explicitly include polarization in the model. However, more studies are required before this is shown to be a general pattern.

Acknowledgment. This project was partially supported by the Kansas Agricultural Experimental Station (Contribution No. 03-267-J). This material is based upon work supported by DOE grant DE-FG02-99ER45764, NSF, and matching support from the State of Kansas. Acknowledgment is made to the donors of the Petroleum Research Fund, administered by the ACS, for partial support of the research.

References and Notes

(1) Tanford, C. *Physical Chemistry of Macromolecules*; John Wiley & Sons: New York, 1961.
(2) Schellman, J. A. *Biopolymers* **1994**, *34*, 1015−1026.
(3) Timasheff, S. N. *Adv. Protein Chem.* **1998**, *51*, 356−432.
(4) Kuharski, R. A.; Rossky, P. J. *J. Am. Chem. Soc.* **1984**, *106*, 5786−5793.
(5) Tirado-Rives, J.; Orozco, M.; Jorgensen, W. L. *Biochemistry* **1997**, *36*, 7313−7329.
(6) Wallqvist, A.; Covell, D. G.; Thirumalai, D. *J. Am. Chem. Soc.* **1998**, *120*, 427−428.
(7) Caflisch, A.; Karplus, M. *Struct. Fold. Des.* **1999**, *7*, 477−488.
(8) Boek, E. S.; Briels, W. J. *J. Chem. Phys.* **1993**, *98*, 1422−1427.
(9) Duffy, E. M.; Severance, D. L.; Jorgensen, W. L. *Isr. J. Chem.* **1993**, *33*, 323−330.
(10) Hernandez-Cobos, J.; Ortega-Blake, I.; Bonilla-Marin, M.; Moreno-Bello, M. *J. Chem. Phys.* **1993**, *99*, 9122−9134.
(11) Åstrand, P. O.; Wallqvist, A.; Karlström, G. *J. Phys. Chem.* **1994**, *98*, 8224−8233.
(12) Tsai, J.; Gerstein, M.; Levitt, M. *J. Chem. Phys.* **1996**, *104*, 9417−9430.
(13) Engkvist, O.; Price, S. L.; Stone, A. J. *Phys. Chem. Chem. Phys.* **2000**, *2*, 3017−3027.
(14) Kallies, B. *Phys. Chem. Chem. Phys.* **2002**, *4*, 86−94.
(15) Chitra, R.; Smith, P. E. *J. Phys. Chem. B* **2001**, *105*, 11513−11522.
(16) Sokolić, F.; Idrissi, A.; Perera, A. *J. Chem. Phys.* **2002**, *116*, 1636−1646.
(17) Chitra, R.; Smith, P. E. *J. Phys. Chem. B* **2002**, *106*, 1492−1500.
(18) Kirkwood, J. G.; Buff, F. P. *J. Chem. Phys.* **1951**, *19*, 774−777.
(19) Berendsen, H. J. C.; Grigera, J. R.; Straatsma, T. P. *J. Phys. Chem.* **1987**, *91*, 6269−6271.
(20) Berendsen, H. J. C.; Postma, J. P. M.; van Gunsteren, W. F.; Hermans, J. Interaction Models for Water in Relation to Protein Hydration. In *Intermolecular Forces*; Pullman, B., Ed.; Reidel: Dordrecht, 1981; pp 331−342.
(21) Jorgensen, W. L.; Chandrasekhar, J.; Madura, J. D.; Impey, R. W.; Klein, M. L. *J. Chem. Phys.* **1983**, *79*, 926−935.
(22) Berendsen, H. J. C.; Postma, J. P. M.; van Gunsteren, W. F.; DiNola, A.; Haak, J. R. *J. Chem. Phys.* **1984**, *81*, 3684−3690.
(23) Ryckaert, J.-P.; Ciccotti, G.; Berendsen, H. J. C. *J. Comput. Phys.* **1977**, *23*, 327−341.
(24) de Leeuw, S. W.; Perram, J. W.; Smith, E. R. *Proc. R. Soc. London A* **1980**, *373*, 27−56.
(25) Darden, T.; York, D.; Pedersen, L. *J. Chem. Phys.* **1993**, *98*, 10089−10092.
(26) Chitra, R.; Smith, P. E. *J. Phys. Chem. B* **2000**, *104*, 5854−5864.
(27) Allen, M. P.; Tildesley, D. J. *Computer Simulation of Liquids*; Oxford University Press: Oxford, 1987.
(28) Smith, P. E.; van Gunsteren, W. F. *J. Chem. Phys.* **1994**, *100*, 577−585.
(29) Ben-Naim, A. *Statistical Thermodynamics for Chemists and Biochemists*; Plenum Press: New York, 1992.
(30) Chitra, R.; Smith, P. E. *J. Chem. Phys.* **2001**, *114*, 426−435.

(31) Chitra, R.; Smith, P. E. *J. Chem. Phys.* **2001**, *115*, 5521−5530.
(32) Swaminathan, S.; Craven, B. M. *Acta Crystallogr.* **1984**, *B40*, 300−306.
(33) van Gunsteren, W. F.; Billeter, S. R.; Eising, A. A.; Hünenberger, P. H.; Krüger, P.; Mark, A. E.; Scott, W. R. P.; Tironi, I. G. *Biomolecular Simulation: The GROMOS96 Manual and User Guid;* vdf Hochschulverlang: ETH Zürich, Switzerland, 1996.
(34) Weerasinghe, S.; Smith, P. E. *J. Chem. Phys.* **2003**, *118*, 5901−5910.
(35) Miller, K. J.; Savchik, J. A. *J. Am. Chem. Soc.* **1979**, *101*, 7206−7213.
(36) Atkins, P. W. *Physical Chemistry*, *2*nd ed.; Oxford University Press: London, 1982.
(37) Hinze, J.; Jaffé, H. H. *J. Am. Chem. Soc.* **1962**, *84*, 540−546.
(38) Dovesi, R.; Causa, M.; Orlando, R.; Roetti, C. *J. Chem. Phys.* **1990**, *92*, 7402−7411.
(39) Gaumann, T. *Helv. Chim. Acta* **1958**, *41B*, 1957−1970.
(40) Finney, J. L.; Soper, A. K.; Turner, J. *Physica B* **1989**, *156 & 157*, 151−153.
(41) Stokes, R. H. *Aust. J. Chem.* **1967**, *20*, 2087−2100.
(42) Miyawaki, O.; Saito, A.; Matsuo, T.; Nakamura, K. *Biosci. Biotechnol. Biochem.* **1997**, *61*, 466−469.
(43) Ben-Naim, A. Inversion of Kirkwood−Buff Theory of Solutions and Its Applications. In *Advances in Thermodynamics. Fluctuation Theory of Mixtures*; Matteoli, E., Mansoori, G. A., Eds.; Taylor & Francis: New York, 1990; Vol. 2, pp 211−226.
(44) *Advances in Thermodynamics. Fluctuation Theory of Mixtures*; Matteoli, E., Mansoori, G. A., Eds.; Taylor & Francis: New York, 1990; Vol. 2.
(45) Robinson, R. A.; Stokes, R. H. *Electrolyte Solutions*; Butterworths: London, 1959.
(46) Smith, P. E.; van Gunsteren, W. F. *J. Chem. Phys.* **1994**, *100*, 3169−3174.
(47) Boek, E. S.; Briels, W. J.; van Eerden, J.; Feil, D. *J. Chem. Phys.* **1992**, *96*, 7010−7018.
(48) Kawahara, K.; Tanford, C. *J. Biol. Chem.* **1966**, *241*, 3228−3232.
(49) Gostling, L. J.; Akeley, D. F. *J. Am. Chem. Soc.* **1952**, *74*, 2058−2060.
(50) Albright, J. G.; Mills, R. *J. Phys. Chem.* **1965**, *69*, 3120−3126.
(51) Wyman, J., Jr. *J. Am. Chem. Soc.* **1933**, *55*, 4116−4121.
(52) Gucker, F. T., Jr.; Gage, F. W.; Moser, C. E. *J. Am. Chem. Soc.* **1938**, *60*, 2582−2588.
(53) Endo, H. *Bull. Chem. Soc. Jpn.* **1973**, *46*, 1106−1111.